Transactions, SMiRT-26
Berlin/Potsdam, Germany, July 10-15, 2022
Division IV

ENHANCEMENT OF SAMMON'S MAP REPRESENTATION OF FAULT RUPTURE MODEL FOR PROBABILISTIC SEISMIC HAZARD ANALYSIS

Masato Nakajima[1] and Norman Abrahamson[2]

[1]Senior Research Associate, Central Research Institute of Electric Power Industry, Abiko-shi, Chiba-ken, Japan (masato@criepi.denken.or.jp)
[2]Adjacent Professor, U.C. Berkeley, Berkeley, CA, USA (abrahamson@berkeley.edu)

ABSTRACT

This paper proposes an improved method for selecting ground-motion models for probabilistic seismic hazard analysis. First, a brief overview of previous selection methods (e.g., Cotton et al.'s method, Scherbaum et al.'s method, South Western United States (SWUS) Senior Seismic Hazard Analysis Committee (SSHAC) Project method) is presented. In this study, we focus on the SWUS's method using Sammon's map representation as we believe that this method is the most rigorous from the viewpoint of mathematics. Then, the approach is analysed for application to numerical simulations of ground motion. Finally, the method using Sammon's map representation is improved so that it can consider cases where the magnitude for candidate ground-motion prediction equations (GMPEs) needs to be unified. There exists strong nonlinearity among the parameters of these equations. It is concluded that the Sammon' map representation method is applicable to fault-rupture model-based simulations for predicting ground motions, and the enhanced Sammon's map provides more detailed information for epistemic uncertainty evaluation with respect to ground-motion models.

INTRODUCTION

The evaluation of epistemic uncertainties is a key issue in probabilistic seismic hazard assessment (PSHA). The Senior Seismic Hazard Analysis Committee (SSHAC) first published NUREG-2117 guideline methodologies in 2012; these have been widely adopted in the US and other countries (e.g., in the Swiss PEGASOS Project). The guidelines proposed by the SSHAC guideline provide a logical and rational procedure to assess epistemic uncertainties that arise from ground-motion characterisation (GMC) and seismic source characterisation (SSC). However, although a few methods and techniques have been developed, certain issues still remain to be addressed when selecting ground-motion models for use in PSHA.

With respect to GMC, it is necessary to build logic trees on the basis of appropriately selected ground-motion models that can represent the ground motion accurately for a target site/area. In general, the backbone approach (e.g., Atkinson (2014)) and the selection-criteria approach (e.g., Cotton et al. (2006)) have been widely used to select ground-motion models, and more quantitative selection methods using information regarding consistency of data (e.g., Scherbaum et al. (2009)) have also been discussed.
The SWUS SSHAC Project (GeoPentech (2015)) developed a novel and innovative selection method for PSHA using a non-linear mapping technique for PSHA on the basis of Scherbaum's work. The method developed can rigorously meet the following necessary and sufficient conditions for building logic trees:

- Logic tree branches are mutually exclusive in the same hierarchy
- Logic tree branches are collectively exhaustive in the same hierarchy

The SSHAC (Senior Seismic Hazard Analysis Committee) guideline methodology published as NUREG-2117 provides a logical and rational procedure of evaluating epistemic uncertainty in PSHA; however, there still exists technical gaps to be addressed in the Seismic Source Characterization (SSC) and Ground-Motion Characterization (GMC). In the NGA-East SSHAC project (2018), the method of epistemic uncertainty evaluation regarding GMMs was enhanced and refined furthermore. This study aims at developing a method to select simulation-based ground-motion models based on fault-rupture models quantitatively by applying the Sammon's Map representation method.

GROUND-MOTION SELECTION METHOD USING SAMMON'S MAP REPRESENTATION

First, we examine ground-motion selection methods using the Sammon's map representation of the alternative magnitude and the site-to-source distance scaling of the GMPEs.

Evaluation of the Ground-Motion Median Model using Sammon's Map Representation

The SWUS SSHAC Project developed a method that makes it possible to select ground motion-models more quantitatively and subjectively. The method employs a nonlinear mapping technique developed by Sammon (1969).

The difference between GMPE i and GMPE j is quantified using Equation (1):

$$E = \frac{1}{\sum_{i<j} \overline{\Delta_{GM}}_{ij}} \cdot \sum_{i<j} \frac{\left(\overline{\Delta_{GM}}_{ij} - \overline{\Delta_{map}}_{ij}\right)^2}{\overline{\Delta_{GM}}_{ij}} \tag{1}$$

where $\overline{\Delta_{GM_{ij}}}$ denotes the distance between the two GMPEs in original high-dimensional space, and $\overline{\Delta_{map_{ij}}}$ denotes the distance in a low-dimensional space that maintains the same relationship in a high-dimensional space. We employ three distance metric, which are defined as follows:

$$\overline{\Delta_{GM_{ij}}}(L_1) = \frac{1}{N}\sum_{k}^{N} \left|\mathrm{GMPE}_{ik} - \mathrm{GMPE}_{jk}\right| \tag{2}$$

$$\overline{\Delta_{GM_{ij}}}(L_2) = \sqrt{\frac{1}{N}\sum_{k}^{N} \left(\mathrm{GMPE}_{ik} - \mathrm{GMPE}_{jk}\right)^2} \tag{3}$$

$$\overline{\Delta_{GM_{ij}}}(L_\infty) = max_k \left|\mathrm{GMPE}_{ik} - \mathrm{GMPE}_{jk}\right| \tag{4}$$

To calculate the distances between candidate GMPEs in probability space, the following steps are applied:

Step 1: Calculate the ground-motion level by GMPEs for a suite of scenarios

The ground-motion level is calculated by the selected GMPE for a set of magnitude M and site-to-source distances R. The faulting type and shear-wave velocity, V_S, are set considering the conditions of the target site and seismic sources.

Step 2: Set the reference ground-motion model

We refer to the average of all ground-motion models as "mix" hereafter. Three indexes are calculated as a reference point from the following equations:

(a)Index regarding the increment/decrement of the predicted value

$$mix + \ln(\alpha) \cdots \alpha = 0.67, 0.8, 1.25, 1.5 \tag{5}$$

The ground-motion values obtained using the scale factor listed above are denoted as $S_{--}, S_{-}, S_{+}, S_{++}$.

(b)Index regarding the sensitivity of the earthquake magnitude

$$mix + \beta(M_w - 6) \cdots \beta = 0.67, 0.8, 1.25, 1.5 \quad (6)$$

The ground-motion values obtained using the magnitude scale factors listed above are denoted as $M_{--}, M_{-}, M_{+}, M_{++}$.

(c)Index regarding the sensitivity of the site to source distance

$$mix + \gamma(R_{JB} - 30) \cdots \gamma = -0.01, -0.005, 0.005, 0.01 \quad (7)$$

The ground-motion values obtained using the linear distance scale factors listed above are denoted as $R_{--}, R_{-}, R_{+}, R_{++}$.

Step 3: Set the axes in the contracted space

The map is centred on the average model at the point (0,0). Then, the map is rotated so that the model S_{++} is to the right, and the line from S to S_{++} is approximately horizontal. Finally, the map is mirrored about the x axis such that M_{++} is located in the upper half of the space (positive y-axis direction).

Step 4: Compute the distance between the candidate GMPEs in the contracted space

Using the equations listed above, the distances between the candidate GMPEs in the contracted space are computed. A set of vectors $X_i (i = 1, \ldots, N)$ is assumed to exist in an L-th dimensional space. This space is referred to as the "Original high-dimensional space" hereafter. The data structure analysis method by Sammon (1969) makes it possible to obtain a set of vectors $Y_i (i = 1, \ldots, N)$ in d -th dimensions (d < L) in a contracted space that has an similar positional relationship as that in the original space. In general, d is set to as 2 or 3 to easily visualise and grasp what the map indicates.

The vector X_i $(i = 1, \cdots, N)$ is assumed to exist in the L-th original high-dimensional space. The objective of the calculation is to search vector Y_i $(i = 1, \cdots, N)$ in a d-th dimensional space that is a two- or three-dimensional space, which is referred to as the "contracted space". We define the distance of each vector as follows:

$$\begin{aligned} \text{Original space: } & d_{ij}^{*} \equiv \text{dist}[X_i, X_j] \\ \text{Contracted (Reduced) space: } & d_{ij} \equiv \text{dist}[Y_i, Y_j] \end{aligned} \quad (8)$$

As an initial d-th dimensional space configuration, we randomly select a Y vector as follows:

$$Y_1 = \begin{bmatrix} y_{11} \\ \vdots \\ y_{1d} \end{bmatrix} \; Y_2 = \begin{bmatrix} y_{21} \\ \vdots \\ y_{2d} \end{bmatrix} \; \ldots \; Y_N = \begin{bmatrix} y_{N1} \\ \vdots \\ y_{Nd} \end{bmatrix}$$

The Y vector assembly is searched that minimises the error E by changing the candidate y_{pq}; $(p = 1, \cdots, N)(q = 1, \cdots, d)$

$$E = \frac{1}{\sum_{i<j} d_{ij}^{*}} \cdot \sum_{i<j}^{N} \frac{\left(d_{ij}^{*} - d_{ij}\right)^2}{d_{ij}^{*}} \quad (9)$$

For example, in a case where we select three GMPEs as a ground-motions models in the two-dimensional space, we set the Y vector assembly as:

$$Y_1 = \begin{bmatrix} y_{11} \\ y_{12} \end{bmatrix} \; Y_2 = \begin{bmatrix} y_{21} \\ y_{22} \end{bmatrix} \; Y_N = \begin{bmatrix} y_{31} \\ y_{32} \end{bmatrix} \quad (10)$$

In a case where there are four GMPEs candidates, the Y vectors are set as follows:

$$Y_1 = \begin{bmatrix} y_{11} \\ y_{12} \end{bmatrix} \; Y_2 = \begin{bmatrix} y_{21} \\ y_{22} \end{bmatrix} \; Y_3 = \begin{bmatrix} y_{31} \\ y_{32} \end{bmatrix} \; Y_4 = \begin{bmatrix} y_{41} \\ y_{42} \end{bmatrix}$$

Step 5: Verify the search algorithm for the optimal solution

It is necessary to verify the computational algorithm when the scaling factor assigns different values to a candidate GMPE. Specifically, the relationship between $\overline{\Delta_{GM_{ij}}}(L_\infty)$ and $\overline{\Delta_{map_{ij}}}(L_\infty)$ is invariant and does not depend on the GMPE.

NUMERICAL SIMULATIONS

Problem Settings of Sammon's Map Representation for Ground-Motion Models

In this paper, we discuss the Sammon's map representation for ground-motion models based on simulations using fault-rupture models. The simulations based on fault-rupture models consist of a greater number of parameters than empirical GMPEs. Therefore, non-linearity of predicted ground motions among candidate simulations methods becomes stronger than for GMPEs. We adopt the Southern California Earthquake Center Broad Band Platform (SCEC-BBP) to simulate ground motions, and Table 1 shows the simulation methods employed in our study. We consider both inland crustal earthquakes and interplate earthquake. The set of fault model parameters vary as shown in Table 2. Other parameters which are required in simulations are set by referring to the parameter values provided in the sample input files for the SCEC-BBP.

Table 1: Ground motion simulation methods adopted in analyses

No.	Module Name	Simulation Method
1	EXSIM	Atkinson and Assatourians (2015)
2	GP	Graves and Pitarka (2015)
3	Irikura	Irikura and Miyake (2001, 2011)
4	SDSU	Olsen and Takedatsu (2015)

Table 2: Parameter settings of seismic sources

Inland crustal earthquake	Dip angle= 90°, fault dimensions and position are modelled to satisfy each case. ● Mw=5.0,5.25,5.5,5.75,6.0,…,7.0,7.25,7.5 (11 patterns) ● R=1,5,10,15,20,25,30,35,…,65,70 km (10patterns)
Interplate earthquake	Fault dimensions and position are modelled to satisfy each case. ● Mw=6.0,5.25,5.5,5.75,6.0,…,7.75,8.0 (11 patterns) ● R=1,5,10,15,20,25,30,35,…,65,70 km (10 patterns)

Advanced Optimization Method

In general, the gradient decent method or the conjugate gradient method has been adopted in conducting optimal solution search. However, those conventional algorithms do not work appropriately from the viewpoint of precision and computational time in the case in which non-linearity is strong. To carry out the calculation of Sammon's Map representation for fault-rupture models, where there exists extensively strong non-linearity among predicted values obtained from each simulation, we employ the Particle Swarm Optimization Method (e.g., Eberhart et al. (1996), Floudas (1987)), denoted as the "PSO method".

First, basic equations are addressed here. Suppose that a problem is prescribed in D–th dimensions, the particle swarm is represented as following vector:

$$X_i = (x_{i1}, x_{i2}, \cdots, x_{iD}) \tag{11}$$

We denote the best particle in the swarm, that has the lowest function, by index "g". The best previous position of the i–th particle is recorded and represented as $P_i = (p_{i1}, p_{i2}, \dots, p_{iD})$, and the position change, namely velocity, of the i-th particle is $V_i = (v_{i1}, v_{i2}, \dots, v_{iD})$.

The particles are manipulated according the following equations:

$$V_i^{k+1} = X\left(wV_i^k + c_1 r_{i1}^k\left(P_i^k - X_i^k\right) + c_2 r_{i2}^k\left(P_g^k - X_i^k\right)\right) \quad (12)$$

$$X_i^{k+1} = X_i^k + V_i^{k+1} \quad (13)$$

where the superscripts denote the iterations, $i = 1,2, \ldots N$ and N denote the size of the populations, χ is a constriction factor that is used to control velocities of the swarm particle, w is the inertia weight and c_1 and c_2 are two positive constants called as cognitive and social parameter, respectively. The algorithm of the PSO method is specifically described as follows:

Step 1: Set positions and velocities of the swarm randomly in a target space and set the number of iterations in conducting the PSO method.

Step 2: Initialize the best solution (position) $\hat{x}_{local}$ locally as the present position.

Step 3: Initialize the particle position which has the highest goodness of fit in the swarm as $\hat{x}_g^{best}$.

Step 4: If the goodness of fit of the $\hat{x}_g^{best}$ is smaller than the criteria and the current loop number is within the setting number, iterate as the follows:

- Renew the position,
- Calculate/measure the goodness of the fit at the renewed position,
- Replace the $\hat{x}_g^{best}$ when its goodness of fit is improved.

Based on the preliminary analyses, we set the weight parameter values as $w = 0.25$, $\rho_{max} = 0.75$ which makes it possible to obtain optimal solutions with the lowest error in the shortest time in a case in which the fault-rupture models shown in Table 1 are employed as ground-motion models. Furthermore, we set the number of iterations at 10000 which can ensure that the error is sufficiently small.

Sammon's Map Representation for Fault Rupture Model: two parameters (M, R)

For crustal earthquakes, we computed ground motions based on fault-rupture models shown in Table 1 using SCEC-BBP Version 19.4 (SCEC, 2020). Next, we calculated the Sammon's Map following the procedure addressed in the previous section. Figure 1 shows the Sammon's Map representation for the fault-rupture model where we adopt a maximum value in the vector composition denoted "AccMaxMag"defined by a maximum value in vector composition. Figures 1 (a-c) show the result of three cases of different distance indices (L_1 norm, L_2 norm, L_∞ norm), respectively. Figure 2 shows the Sammon's Map representation for fault-rupture model where we adopt a maximum value of the two horizontal components denoted as "AccMax". The results represented by the Sammon's Map indicate the following issues:

- The Sammon's Map of the fault-rupture model with distance index of L_1 norm and L_2 norm are similar when the same number of particles are adopted, whereas, the Sammon's Map with distance index L_∞ norm has different features than the L_1 norm and L_2 norm maps. .
- We can safely address that epistemic uncertainty between GP and Irikura is small. It should be noted that SDSU and EXSIM has a characteristic position in epistemic uncertainty evaluation because those three simulations are positioned with a certain distance in different quadrant in the Sammon's Map.
- The Sammon's Map where a position of each fault rupture model in probabilistic space is shown differs when we adopt AccMaxMag or AccMax as a representative value of simulated ground motion. Fault rupture model-based simulations make it possible to provide three components. Therefore, selection of target component is also key issue.

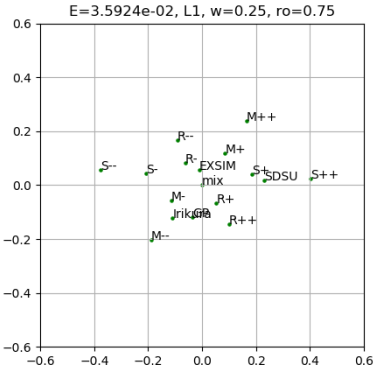

(a)Distance index: L_1 norm

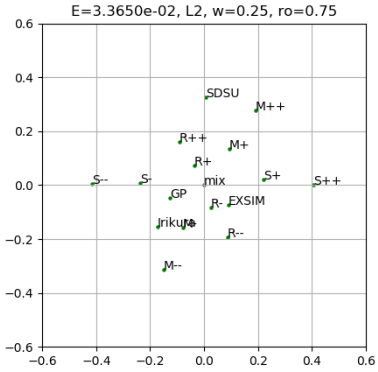

(b)Distance index: L_2 norm

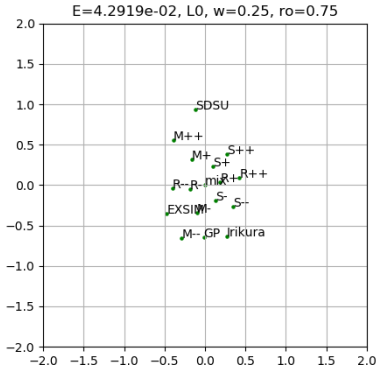

(c)Distance index: L_∞ norm

Figure 1. Sammon's Map Representation of Fault-Rupture Models using five simulation methods available in the SCEC-BBP listed in Table 1.
[Component: AccMaxMag, number of particles: 10000]

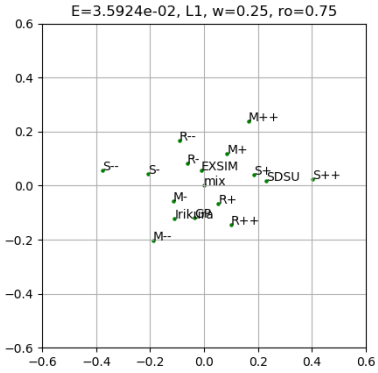

(a)Distance index: L_1 norm

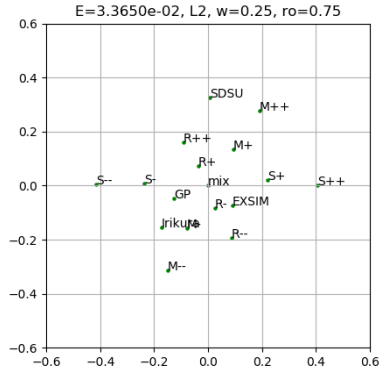

(b)Distance index: L_2 norm

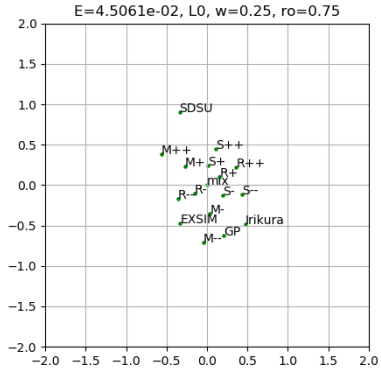

(c)Distance index: L_∞ norm

Figure 2. Sammon's Map Representation of Fault Rupture Model
[Component: AccMax, number of particles: 10000]

Enhanced Sammon's Map Representation for Fault Rupture Model: three parameters ($M, R, \Delta\sigma$)

There are three main differences in the ground-motions from the different simulation methods: constant shift, magnitude scaling, and distance scaling. The original Sammon's Map method is evaluated for scenarios that sample two parameters: magnitude M and the source-to-site distance R. This is because peak value of ground motion is mainly determined by those two parameters. However, other parameters than magnitude and source- to-site distance can affect the result, which is caused by outer and inner parameters of fault-rupture models. Here, we develop Sammon's Map representation using scenarios with three parameters:magnitude M, source-to-site distance R, and stress drop $\Delta\sigma$. Using a different median stress drop measures epistemic uncertainty regarding median ground motion evaluated based on fault rupture model (i.e., it is a scale factor). In this analyses, interplate earthquakes are considered, and we set the cases to be used as follows:

Step 0: The M and R are set as shown in Table 2.

Step 1:The fault area S and moment magnitude M_0 are determined based on fault dimension and relevant parameter values. Stress drop is evaluated based on the following equation:

$$\Delta\sigma = 2.5 \times M_0 / S^{3/2} \tag{14}$$

Here, the seismic moment,M_0, is determined from the moment magnitude M.

Step 2: Assume that variability of stress drop $\Delta\sigma$ is modelled based on a normal distribution (Gaussian) with COV=0.7 as following equation:

$$\mathrm{COV}\left(=\frac{\zeta}{\mu}\right)=0.7 \tag{15}$$

where μ and ζ denotes mean and standard deviation, respectively.

Step 3: As shown in Table 3, five points are selected from the probability distribution determined in Step 2.

Table 3: Calculation case of stress drop $\Delta\sigma$

Parameter	Calculation case
$\Delta\sigma$	$\mu-\zeta,\ \mu-0.5\zeta, \mu,\ \mu+0.5\zeta, \mu+\zeta$

Step 4: Ground motions (time-history waveforms) are simulated based on the fault-rupture models shown in Table 1. Then, the peak acceleration value is identified for each case. We define that the values obtained above are denoted as $SD_{--}, SD_{-}, SD_{+}, SD_{++}$.

Figure 3 (a-c) and 4 (a-c) show Sammon' map represented by M, R, Δ.

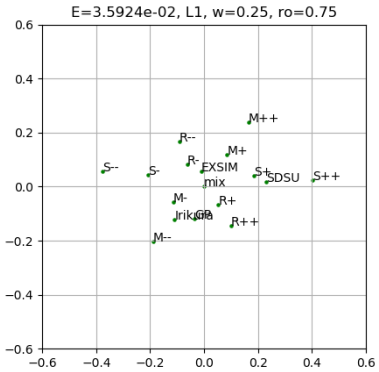

(a)Distance index: L_1 norm

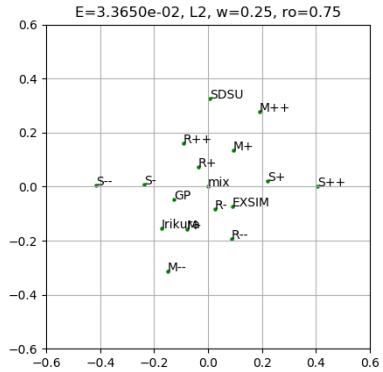

(b)Distance index: L_2 norm

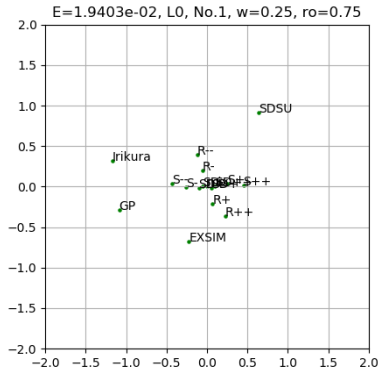

(c)Distance index: L_∞ norm

Figure 3. Sammon's Map Representation of Fault Rupture Model using $(R, \Delta\sigma)$
[Component: AccMaxMag number of particles: 10000]

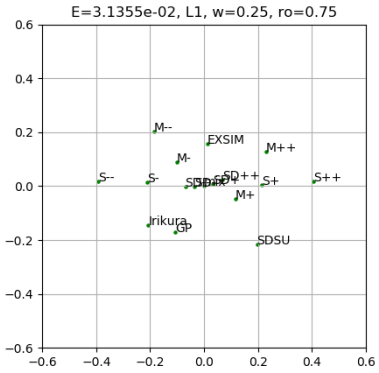

(a)Distance index: L_1 norm

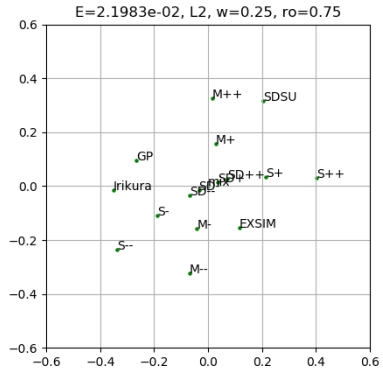

(b)Distance index: L_2 norm

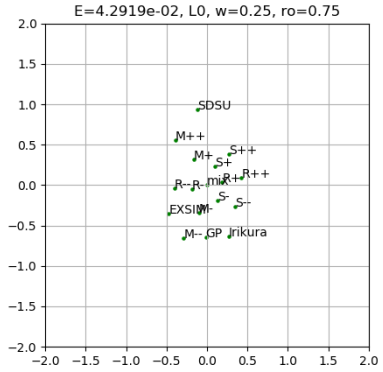

(c)Distance index: L_∞ norm

Figure 4. Sammon's Map Representation of Fault Rupture Model using $(M, \Delta\sigma)$
[Component: AccMaxMag, number of particles: 10000]

DISCUSSIONS

Through case study analysis based using numerical simulations, we found the following features of Sammon's Map representation for fault rupture models.

We have to inquire, to some extent, into uncertainties induced variations of the Sammon's map.

- The Sammon's Map where a position of each fault rupture model in probabilistic space is shown differs when we adopt AccMaxMag or AccMax as a representative value of simulated ground motion. Fault-rupture-model-based simulations make it possible to provide three components. Therefore, selection of target component is also key issue.
- The space size of Sammon's Map representation using three parameters is larger than that using original two parameters, indicating that the simulation methods scale differently with stress drop. We can safely say that it is a natural result because positional relationship in Sammon's Map representation is evaluated based on combination of greater number of calculation cases.
- We can capture detailed features of ground motion by adopting fault rupture model-based simulation. In order to utilize fault-rupture model in PSHA, a probability distribution model to represent the uncertainty should be specifically discussed because fault rupture model consists of greater number of parameters compared to GMPEs, and some parameters greatly affect the simulation results (e.g., time history waveform, response spectrum, Fourier spectrum).
- We need to investigate a case of Sammon's Map representation where both GMPEs and fault-rupture models are candidates as GMMs.

Although it is derived from a limited number of calculation results, we want to stress that epistemic uncertainty of GMM based on fault-rupture models can be assessed in the Sammon's Map representation as same as GMM based on GMPEs. Furthermore, it is necessary to examine the effect of the variation of Sammon's map representation on the weight value, which is obtained using the residual and likelihood. We have already obtained the Sammon's Map representations with other combination of three parameters (e.g., magnitude M, site-to-source distance R and rupture velocity V_r). Some of additional examinations will be presented in the conference.

CONCLUSION

We expanded the Sammon's Map representation for ground motion model to fault rupture models, and illustrated several examples based on numerical simulations. Conclusions obtained from this study are summarized as follows:

(1) Quantitative selection method of ground-motion models is enhanced. Specifically, we upgrade the Sammon's Map representation method to apply to fault rupture models.
(2) We discuss a method to evaluate uncertainties in a case where several alternative fault-rupture models can be employed in the GMC. The improved method makes it possible to select applicable fault-rupture models and develop weights for the logic tree branches quantitatively by sampling the space covered by the Sammon's Map. This leads to improved epistemic uncertainties in conducting PSHA in a case where the dominant seismic source is located close to a site and prediction of near-field ground motion can affect the seismic hazard evaluation.

REFERENCES

Atkinson, G.R., Bommer, J.J. and Abrahamson, N. (2014). "Alternative approaches to modelling epistemic uncertainty in ground motions in probabilistic seismic-hazard analysis", *Seismological Research Letter*, 85(6), 1141-1144, doi: 10.1785/0220140120.

Atkinson, G. M., and Assatourians, K. (2015) "Implementation and Validation of EXSIM (A Stochastic Finite-Fault Ground-Motion Simulation Algorithm) on the SCEC Broadband Platform", *Seismological Research Letters*, January/February 2015, v. 86, p. 48-60, First published on December 17, 2014, doi:10.1785/0220140097

Cotton, F., Sherbaum, F., Bommer, J.J. and Bungun, H. (2006). "Criteria for selecting and adjusting ground-motion models for specific target regions: Application to Central Europe and rock sites", *Journal of Seismology*, **10**: pp.137-156.

Eberhart, R.C., Simpson, P.K. and Dobbins, R.W. (1996). "Computational Intelligence PC Tools". Academic Press Professional, Boston.

Floudas, C.A., Pardolos, P.M. (1987) "A Collection of Test Problems for Constrained Global Optimization Algorithms" Lecture Notes in Computing Science, Col. 455, Springer-Verlag, Berlin Heidelberg New York.

GeoPentech (2015). "Southwestern United States Ground Motion Characterization SSHAC Level 3", Technical Report, Revision 1

Graves, R., and Pitarka, A. (2015) "Refinements to the Graves and Pitarka (2010) Broadband Ground-Motion Simulation Method", *Seismological Research Letters*, January/February 2015, v. 86, p. 75-80, First published on December 17, doi:10.1785/0220140101

Irikura, K. and Miyake, H. (2001, 2011) "Recipe for Predicting Strong Ground Motion from Crustal Earthquake Scenario", *Pure and Applied Physics*, 168, pp.85-104

Olsen, K. B., and Takedatsu, R. (2015) "The SDSU Broadband Ground-Motion Generation Module BBtoolbox Version 1.5", *Seismological Research Letters*, January/February 2015, v. 86, p. 81-88, First published on December 17, 2014, doi:10.1785/0220140102

Pacific Earthquake Engineering Research Center, (2018). Central and Eastern North America Ground-Motion Characterization NGA-East Final Report, PEER Report No.2018/08

Pacific Gas and Electric Company (2018). "Seismic Probabilistic Risk Assessment in Response to 50.54 (f) Letter with Regard to NTTF 2.1: Seismic Summary Report", Enclosure 1, PG&E Letter DCL-19-027.

Press, W.H., Teukolsky, S.A., Vetterling, W.T. and Flannery, B.P. (1996). "Numerical Recipes in Fortran 90 –The Art of Parallel Scientific Computing-, *Cambridge University Press*"

Sammon, J.W. (1969). "A Nonlinear Mapping for Data Structure Analysis", *IEEE Transactions on Computers*, Vol. **C-18** (5), pp.401-409

SCEC-BBP. https://strike.scec.org/scecpedia/Broadband_Platform

Scherbaum, F., Delavaus, E. and Riggelesen, C. (2009). "Model Selection in Seismic Hazard Analysis: An Information-Theoretic Perspective", *Bulletin of the Seismological Society of America*, Vol. 99, No. 66, pp.3234-3246, 2009.

U.S.NRC (2012). "Practical Implementation Guidelines for SSHAC Level 3 and 4 Hazard Studies", NUREG-2117, Rev.1